Effects of Elastic Deformation on Phase Separation of a Polymer Blend Driven by a Reversible Photo-Cross-Linking Reaction

Xuan-Anh Trinh, Junko Fukuda, Yoshikuni Adachi, Hideyuki Nakanishi, Tomohisa Norisuye, and Qui Tran-Cong-Miyata*

Department of Macromolecular Science and Engineering, Graduate School of Science and Technology, Kyoto Institute of Technology, Matsugasaki, Kyoto 606-8585, Japan

Received March 2, 2007; Revised Manuscript Received May 11, 2007

ABSTRACT: Phase separation driven by a reversible photo-cross-linking reaction was investigated by using anthracene-labeled polystyrene/poly(vinyl methyl ether) (PSA/PVME) blends. Upon irradiation with 365 nm ultraviolet light, anthracene moieties undergo photodimerization, leading to phase separation of the two polymers. On the other hand, the homogenization process of the phase-separated blend was induced by irradiation with 297 nm which converted photodimer back to anthracene monomer, thus de-cross-linking the PSA networks in the mixture. The kinetics of phase separation and the corresponding homogenization processes driven by these two UV wavelengths were followed in situ under a light scattering instrument equipped with a UV light source. Unlike the conventional kinetics of phase separation in nonreacting mixtures, it was found that the scattering peak shifts toward the side of larger wavenumber as phase separation proceeds under 365 nm light. The local elastic deformation of the blend monitored along the course of irradiation by Mach−Zehnder interferometry reveals a strong correlation between the cross-link-induced elastic deformation and the shift of the scattering peak observed during irradiation. On the other hand, the homogenization process of the cross-linked blends was observed upon irradiation with 297 nm. The scattering intensity decreases while the position of the scattering peak remains unchanged with irradiation time. These experimental results do not only provide basic information for modeling reaction-induced phase separation but also would suggest a method for recycling multicomponent polymer blends by taking advantages of UV-induced reversible phase separation.

Introduction

Generation and reversible control of ordered structures in polymeric systems are not only indispensable for technological applications such as fabrication of erasable memories[1] but also important for the understanding of the generic mechanism and the functions of various assembling structures spontaneously emerging in living systems.[2] Compared to thermally activated reactions, photochemical reactions are, in general, more selective, and their potential applicability has been demonstrated over a wide range of controlling molecular structures as well as their assemblies.[3] Among these photochemical reactions, reversible photoisomerization of azobenzene derivatives has been extensively utilized to manipulate various molecular assemblies as well as electrooptical properties of polymers.[4,5] However, the spontaneous *cis* → *trans* photoisomerization of azobenzene and derivatives that occurs at moderate temperatures[6] creates a drawback for the control using light over a wide range of temperature. To overcome this spontaneous process, we have utilized the more stable *trans* → *cis* photoisomerization of stilbene to manipulate the reversibility of phase separation and compared the experimental data with theoretical prediction for phase separation kinetics driven by reversible reactions.[7] However, the reversible photoisomerization of *trans*- ↔ *cis*-stilbenes also has two drawbacks. First, instead of returning to the *trans*-isomer via photoisomerization, the *cis*-stilbene isomer could be changed to an intermediate compound via which the more stable phenanthrene is prominently produced in the presence of oxygen or iodine.[8] The second drawback of photoisomerization of stilbene is the large overlap between the absorption spectra of *trans*- and *cis*-isomers that limits the reversibility of the reaction upon switching irradiation wavelengths. As a consequence, more accessible photoreactions are desirable to achieve the reversible control for phase separation of polymer blends.

From the viewpoint of polymer reactions kinetics, most of chemical reactions promote inhomogeneously in the bulk state of polymers because of the inherent inhomogeneity of their local structures.[9−11] This effect is even more significant for reactions governed by polymer mobility such as diffusion-controlled reaction.[12] As a result, modifying chemical structure of polymer chains in the bulk state by using chemical reactions would lead to the formation of local inhomogeneity via which a local strain field can be generated and developed inside the cross-linked polymer mixture during irradiation. Depending on the irradiation conditions, this strain field may not completely relax during the course of the reaction as directly revealed in recent experiments using Mach−Zehnder interferometry.[13] This coupling occasionally leads to the broadening of the characteristic length scales distribution resulting from the spinodal decomposition process. It has been shown that the regularity of the morphology can be enhanced by relaxing this elastic strain in periodic irradiation experiments.[14]

In this paper, we report the experimental results on reversibly driving phase separation of a binary polymer blend by using two UV wavelengths. First, the reversible photo-cross-link kinetics was monitored and analyzed for the mixture anthracene-labeled polystyrene (PSA) and poly(vinyl methyl ether) (PVME) in the one-phase region. Subsequently, the phase separation process of a PSA/PVME (20/80) blend was followed by using light scattering upon irradiation with 365 nm UV light. The elastic strain field generated by the inhomogeneity of the photo-cross-link reaction was in situ monitored under the same irradiation conditions by using Mach−Zehnder interferometry. The correlation between the phase separation kinetics and the

* To whom correspondence should be addressed. E-mail: qui@kit.ac.jp.

10.1021/ma0705220 CCC: $37.00
Published on Web 06/23/2007

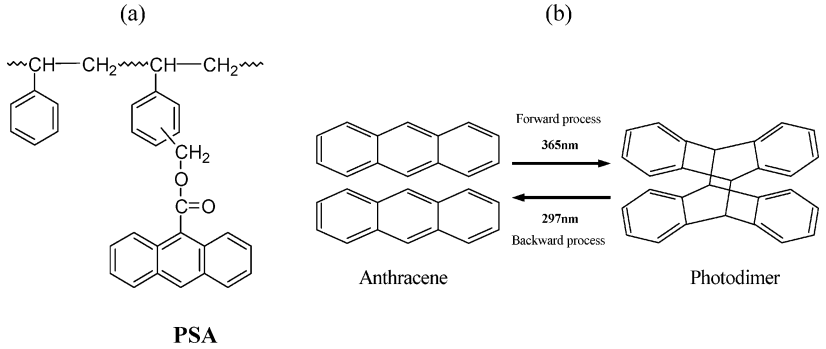

Figure 1. (a) Chemical structure of anthracene-labeled polystyrene (PSA). (b) Reversible photodimerization of anthracene.

relaxation of the deformation induced by cross-link reaction was discussed. The homogenization kinetics induced by photodissociation of anthracene photodimers under irradiation with 297 nm was also described in conjunction with the interferometric data obtained for the phase-separated PSA/PVME blends. Finally, the possibility of "photorecycling" for phase-separated polymer blends will be briefly discussed.

Experimental Section

Sample Preparation. Samples used in this work are the mixtures of anthracene-labeled polystyrene (PSA) and poly(vinyl methyl ether) (PVME). These polymers were prepared according to the method reported previously.[15] Briefly, PSA ($M_w = 2.6 \times 10^5$; $M_w/M_n = 2.2$) was prepared from the precursor polystyrene-*ran*-poly(chloromethylstyrene) copolymer synthesized by free radical polymerization of styrene and chloromethylstyrene (Tokyo Kaisei Inc.). The copolymer was reacted with potassium salt of anthracenecarboxylic acid (Aldrich Chemicals, recrystallized twice in ethanol before use) in dimethylformamide. The label content of PSA is 1 anthracene/52 monomers as determined by using a UV−vis photometer (Shimadzu, model UV-1600). PVME (SP2 Inc., $M_w = 1.0 \times 10^5$; $M_w/M_n = 1.8$) was purified using toluene as good solvent and *n*-heptane as nonsolvent. PSA/PVME (20/80) blends with the thickness 10 μm were prepared by the solvent-casting method and were dried under vacuum with the conditions reported previously. The chemical structure of the polymer PSA used in this study is shown in Figure 1 together with the reversible photodimerization of the photo-cross-linker anthracene.

Reversible Photodimerization Kinetics of Anthracene. PSA/PVME (20/80) blend was irradiated in the one-phase region at 80 °C by using a high-pressure Hg−Xe lamp (350 W/cm^2, Moritex, Japan). To investigate the reversible photodimerization kinetics of anthracene labeled on the PSA component, a PSA/PVME (20/80) blend was irradiated with 365 nm to induce the dimerization of anthracene in the forward process and subsequently by 297 nm to dissociate the photodimer to the anthracene monomer in the backward process. These wavelengths belong to specific line spectra of a Hg−Xe lamp (350 W, Moritex, Japan) and were selected by using appropriate band-pass filters for excitation. The reversible photodimerization induced by these wavelengths is illustrated in Figure 1b. The change in absorbance of anthracene at 365 nm in a PSA/PVME (20/80) blend was monitored by using a UV−vis spectrophotometer (model UV-1600, Shimadzu Inc., Japan) after different intervals of irradiation time. The detailed analysis of the reaction kinetics is described below.

Glass Transition Temperature (T_g). The glass transition temperature of the PSA/PVME (20/80) blend was measured by using differential scanning calorimetry (DSC-3100, MAC Science Inc.) with a heating rate of 10.0 °C/min. The midpoint transition was used to determine the glass transition temperature of the blend.

Light Scattering Experiments. The cloud point of PSA/PVME (20/80) blends was obtained by monitoring the light scattering intensity at a fixed angle while the temperature of the blend was increased with a constant heating rate of 0.2 °C/ min. The cloud point for this particular composition was found as 118.6 °C. The

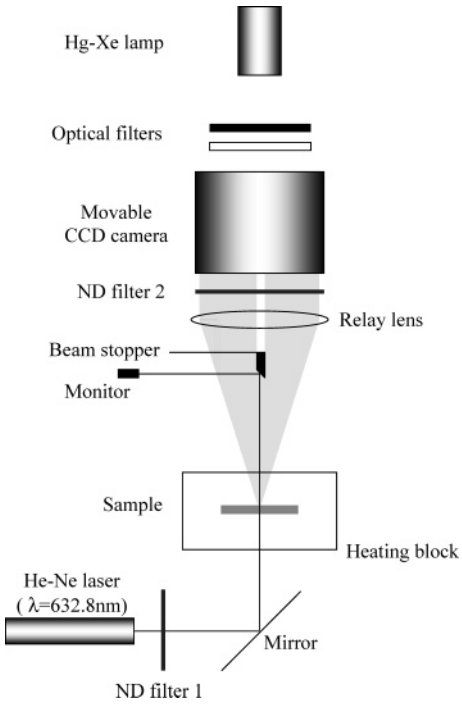

Figure 2. Block diagram of the light scattering instrument equipped with a high-pressure Hg−Xe lamp used in this study.

light scattering profile from a PSA/PVME (20/80) blend was in situ monitored by using a light scattering photometer (Dyna-3000, 632.8 nm, Otsuka Electronics, Japan) equipped with a high-pressure Hg−Xe lamp (350 W, Moritex, Japan). Irradiation was performed with two UV lines 365 and 297 nm of a UV lamp through an optical fiber. As shown in Figure 2, the exciting UV light is set perpendicularly to the surface of a PSA/PVME (20/80) blend that is placed horizontally in a heating block with temperature thermostated with a precision of ±0.5 °C. The scattering profile was detected at the scattering angle ranging from −20° to + 20° by using a 2-dimensional high-sensitivity movable CCD camera (Princeton Instruments Inc.) at 110 °C. The 1-D scattering profile was obtained by circularly averaging the 2-D scattering intensity distribution. The correction for refractive index was performed according to the procedure described by Stein and Keane.[16] From the transmission data of the blend measured after different irradiation time intervals using the same scattering instrument, it was found that the contribution of the sample cloudiness to the scattering intensity is negligible.

Measurements of Elastic Deformation by Mach−Zehnder Interferometry. The principle as well as the instrument was described in detail elsewhere.[13] In brief, a He−Ne laser (10 mW, 362.8 nm, NEC) as a light source was enlarged and collimated before entering a Mach−Zehnder interferometer unit composed of two reflecting and two half mirrors. The interference patterns of the test beam and the reference beams were monitored by using a CCD camera (Tokyo Electronic Industries Co., model CS-8330B)

and stored on a laptop computer (La Vie G, Intel Pentium M Processor 1.0 GHz, NEC). The information on the phase change was calculated from the interference patterns between the test and reference laser beams using Hilbert transform as described previously. The photo-cross-link reaction results in two antagonistic effects in the optical properties of the reacting blend. One is the increase in the refractive index of the sample due to the volume contraction of the blend induced by irradiation cross-link, and the other is the decrease in refractive index caused by the destruction of the π-electron conjugation of anthracene. The optical path length obtained from the interference fringes is a function of both the deformation d and the refractive index n of the blend. Before irradiation, the optical path length OPL_{before} is given by

$$OPL_{before} = \Delta\phi/q = (n-1)d \quad (1)$$

Here, $\Delta\phi$, q, and d represent respectively the phase difference, the wavenumber, and the initial thickness of the blend. In general, upon photo-cross-link, the thickness d and the refractive-index n of the cross-linked blend change to $(d + \Delta d)$ and $(n + \Delta n)$, respectively. The optical path length observed after irradiation over a period of time is then given by

$$OPL_{after} = \Delta\phi_{after}/q = (n + \Delta n)(d + \Delta d) - 1(d + \Delta d) \quad (2)$$

The factor 1 in the front of the last term of eq 2 represents the refractive index of air and n is the refractive-index of the blend. Change in the refractive index Δn of the blend before and after irradiation was directly measured by using the prism-coupling method.[17] It was found that Δn is negligibly small (less than 0.02%) under the experimental conditions of this study.[18] From eq 2, the change in the optical path length (OPLD) of the blend before and after irradiation is approximately given by

$$OPLD = OPL_{after} - OPL_{before} \cong \Delta d(n-1) \quad (3)$$

where $n \cong 1.4871$ is the refractive index of the PSA/PVME (20/80) blend at the experimental temperature (25 °C). Thus, the information on the elastic deformation of the cross-linked blend defined as $\Delta d/d$ is finally given by

$$\frac{OPLD}{d} = OPL_{after} - OPL_{before} \cong (n-1)\frac{\Delta d}{d}$$

or

$$\frac{\Delta d}{d} = \frac{OPLD}{d(n-1)} \quad (4)$$

for various irradiation conditions provided that d, the initial thickness of the blend, is known.

Refractive Index Measurements by Total Internal Reflection. The refractive index of a PSA/PVME (20/80) blend was measured on a prism-coupler (Metricon Corp., model 2010) at 25 °C using a He−Ne laser (632.8 nm) as a light source. The refractive index of the blend n_s was calculated from the total internal reflection principle using the refractive-index of the prism n_p and the corresponding critical angle θ_c measured by the prism coupler:

$$\theta_c = \sin^{-1}\left(\frac{n_s}{n_p}\right) \quad (5)$$

Thus, with n_p known beforehand and the critical angle θ_c obtained from the sudden change in the reflection intensity with the rotating angle of the sample, the refractive index n_s of the blend at 632.8 nm can be calculated.

Results and Discussion

Phase Behavior and Glass Transition Temperature of PSA/PVME Blend. The cloud point (T_{cl}) measured by light scattering and the glass transition temperature (T_g) obtained by DSC for the PSA/PVME blend are illustrated in Figure 3. The blend exhibits a lower critical solution temperature (LCST) as the unlabeled polystyrene/poly(vinyl methyl ether) mixture, except that the cloud point slightly shifts toward the side of low temperature, indicating that introducing anthracene into polystyrene chains worsens the miscibility of the "mother" blend. All the irradiation experiments were performed at 110.0 °C which is located in the one-phase region between the T_{cl} and T_g curves.

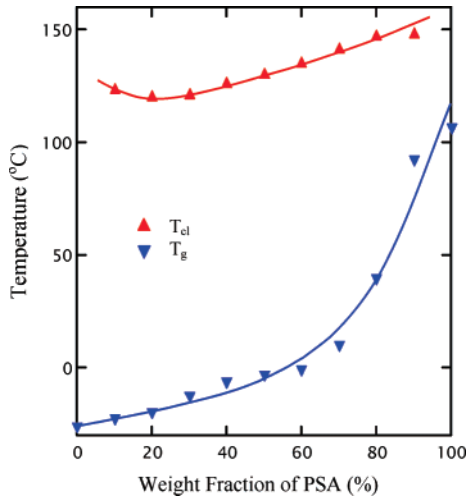

Figure 3. Composition dependence of the cloud point (T_{cl}) and the glass transition temperature (T_g) of the PSA/PVME blend.

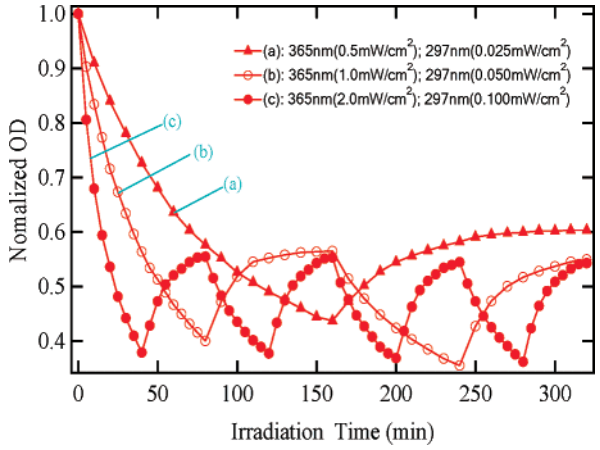

Figure 4. Reversible dimerization kinetics of anthracene in a PSA/PVME (20/80) blend alternatively irradiated with 365 and 297 nm UV light in the one-phase region at 80 °C. Three sets of intensity (365 nm/297 nm) were used for irradiation: (a) 0.5/0.025, (b) 1.0/0.05, and (c) 2.0 mW/cm²/0.1 mW/cm².

Reversible Photodimerization Kinetics of Anthracene in PSA/PVME Blend. Figure 4 shows the variation with irradiation time observed for the absorbance of anthracene moieties in a PSA/PVME (20/80) blend upon alternative irradiation with two wavelengths 365 and 297 nm at 80 °C. It is worth noting that irradiation at this temperature does not have enough ability to bring the blend into the unstable region, and therefore the sample remains in the one-phase region after irradiation. To examine the reversibility of this reaction, the blend was alternatively irradiated with two wavelengths 365 and 297 nm over three equal time intervals $\Delta t = 40$, 80, and 160 min using three sets of light intensity (I_{365}/I_{297} = 2.0/0.1 mW/cm², 1.0/0.05 mW/cm², and 0.5/0.025 mW/cm²). The rates of both the photodimerization (the forward process) and the photodissociation (the backward process) of anthracene induced respectively by 365 and 297 nm UV light increase with increasing

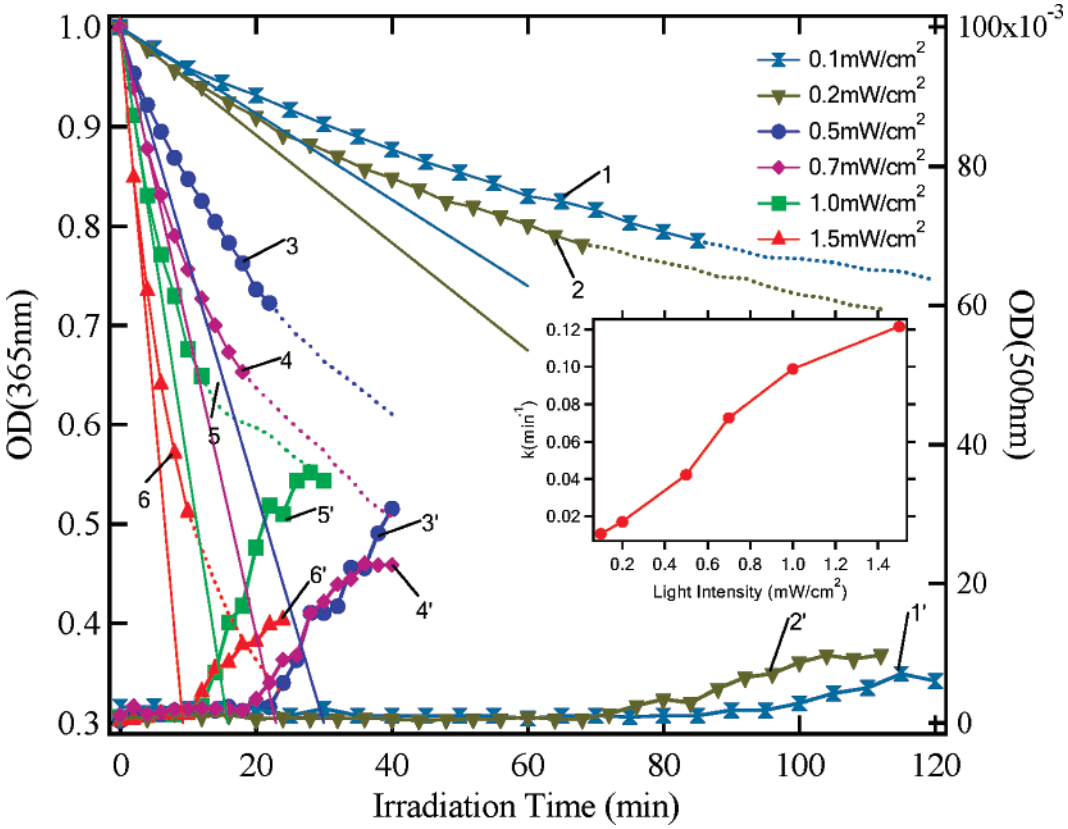

Figure 5. Upper part: photo-cross-link kinetics of PSA/PVME (20/80) blends obtained by irradiation with 365 nm at 110 °C under six intensities: (1) 0.1, (2) 0.2, (3) 0.5, (4) 0.7, (5) 1.0, and (6) 1.5 mW/cm^2. Lower part: the corresponding absorbance of the same blends monitored at 500 nm. Inset: light intensity dependence of the initial slope k calculated from the time-evolution of absorbance.

the irradiation intensity. Obviously, for lower irradiation intensity, the change in the absorbance of anthracene becomes slower with irradiation time. Furthermore, the absorbance monitored at 365 nm is almost recovered (ca. 98%) after irradiation with 297 nm over several photodimerization/photodissociation cycles. The period of reversibility becomes longer for weaker irradiation intensity. To analyze the kinetics of photo-cross-link induced by the dimerization of anthracene, the irradiation time dependence of the absorbance at 365 nm (the forward process) was monitored under several light intensities ranging from 0.1 to 1.5 mW/cm^2. As shown in Figure 5, the decay of the absorbance monitored at 365 nm for a PSA/PVME (20/80) blend irradiated at 110 °C deviates from the decay course at a particular irradiation time as indicated by the dotted lines. This particular point coincides with the irradiation time at which the absorbance of the blend monitored at 500 nm suddenly increases. It is worth noting that the absorbance of anthracene at 500 nm is negligible. Furthermore, the irradiation time corresponding to this deviation increases with decreasing the light intensity, suggesting that this specific change corresponds to the onset of phase separation induced by the photodimerization of anthracene. Since the decay process of the absorbance is interrupted by this phase separation, instead of fitting these experimental results to some model functions of reaction kinetics, the initial slope k defined as $k = \lim_{t\to 0} \mathrm{d[OD}(t)]/\mathrm{d}t$ for the decay curves was calculated and used as a measure for the rate of the cross-link reaction. The dependence of k on the irradiation intensity is illustrated in the inset of Figure 5, showing that the initial slope k increases with increasing the irradiation intensity.

Light Scattering Data of Photo-Cross-Linked Blends. The one-dimensional light scattering profile obtained after circularly averaging the two-dimensional data is shown in Figure 6 for a PSA/PVME (20/80) blend cross-linked at 110 °C under 365 nm UV light with the intensity $I = 0.2$ mW/cm^2. The scattering intensity profiles in situ monitored over different irradiation time exhibit a peculiar behavior. The scattering intensity increases with irradiation time, indicating that phase separation was induced by the cross-link reaction. The broad scattering peak that reveals the presence of modulated structures inside the irradiated blend moves toward the side of larger wavenumber. This behavior is distinctively opposite to the behavior of phase separation often observed for nonreacting mixtures. Shown in Figure 7 is the irradiation time dependence of the wavenumber q_{max} corresponding to the maximum scattering intensity $I(q_{max})$. Here, the peak position was determined from the condition $\mathrm{d}I(q)/\mathrm{d}q \rightarrow 0$. Obviously, q_{max} gradually increases with irradiation time and eventually reaches a stationary state at ca. 250 min of irradiation. These results show that the PSA/PVME (20/80) blend becomes unstable upon cross-link and undergoes phase separation around 40 min after irradiation with UV light with the intensity 0.2 mW/cm^2. The initial characteristic length scale emerges as the blend enters the unstable region and subsequently decreases as irradiation time increases. The dependence of the morphological length scales on irradiation time is somewhat unusual compared to the conventional phase separation kinetics observed by light scattering for nonreacting systems.[19] The irradiation time dependence of the characteristic length scale ξ calculated from the Bragg's law $\xi = 2\pi/q_{max}$ is depicted in Figure 8 for six irradiation intensities ranging from 0.1 to 1.5 mW/cm^2. Here, instead of the irradiation time t_{irr}, the "net" time of phase separation ($t_{irr} - t_0$) was used, where t_0 is the threshold of irradiation time required for the onset of phase separation. This particular time t_0 was defined as the specific time at which the scattering intensity from the irradiated blend exhibits a sudden change upon increasing irradiation time. The data

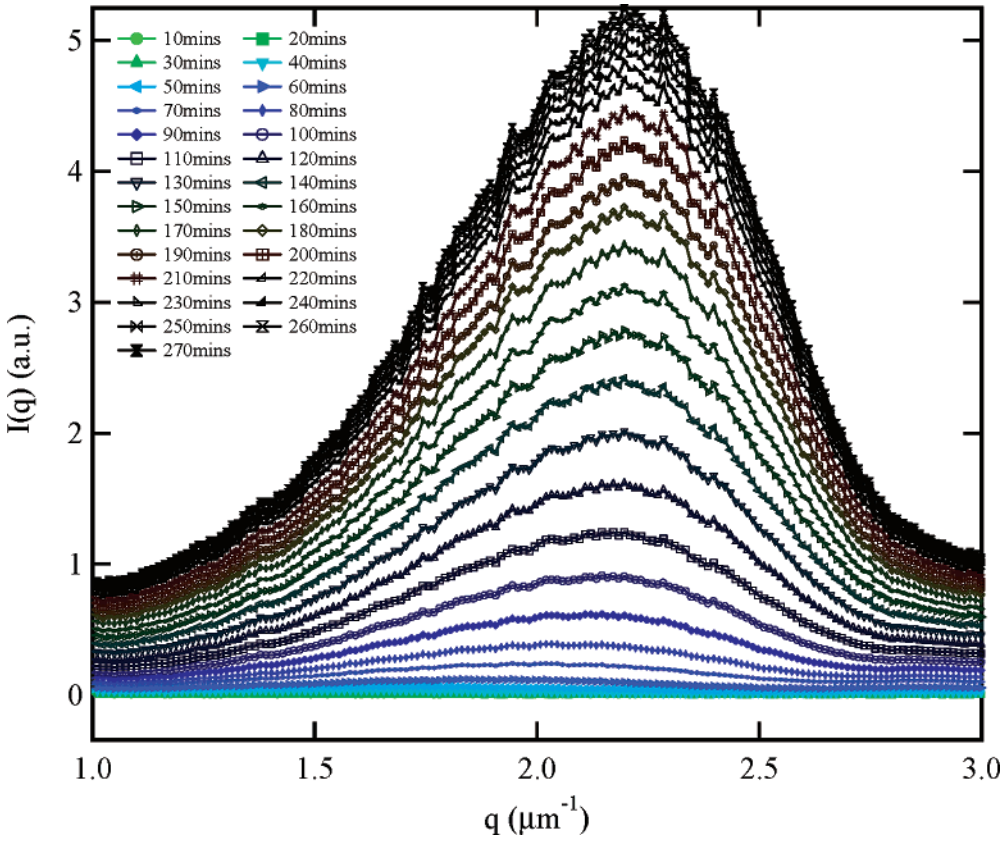

Figure 6. Time evolution of the light scattering intensity observed for the forward phase separation process of a PSA/PVME (20/80) blend induced by 365 nm at 110 °C. Irradiation intensity is 0.2 mW/cm^2.

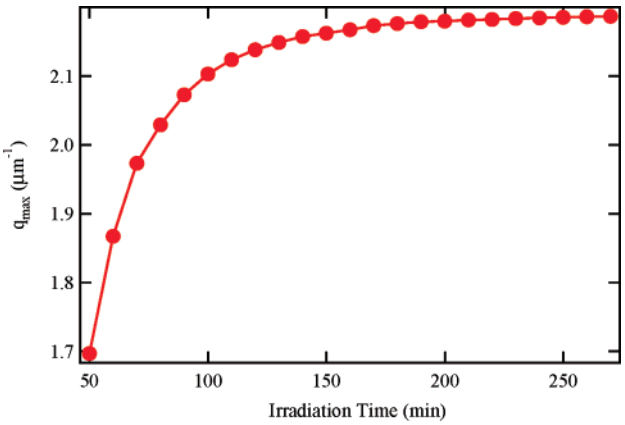

Figure 7. Irradiation time evolution of the scattering peak q_{max} obtained from the data shown in Figure 6.

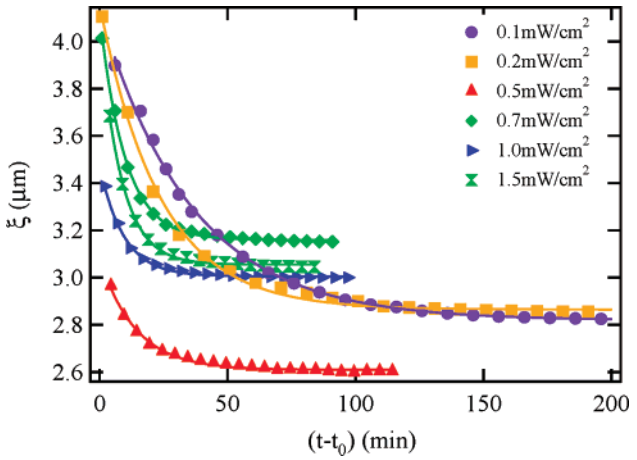

Figure 8. Time evolution of the characteristic length scale observed for a PSA/PVME (20/80) blend irradiated with various light intensities at 110 °C.

obtained for six irradiation intensities share a common behavior as seen in Figure 8. As the "net" irradiation time $\Delta t = (t - t_0)$ increases, the characteristic length scale ξ decreases and eventually reaches a limit at long irradiation time Δt. Upon increasing the irradiation intensity, the decrease in the length scale ξ with Δt appears weaker from a certain intensity. On the other hand, the maximum scattering intensity $I(q_{max})$ corresponding to the wavenumber q_{max} increases with irradiation time and eventually tends to approach a limit at long time as illustrated in Figure 9, indicating that the inhomogeneity of the blend was induced and gradually frozen by the photo-cross-link reaction.

Phase separation of reacting polymer mixtures is the extremely complicated phenomena. Relevant theories are currently not yet established even in the linear region because the mutual couplings among the nonlinear kinetics of the evolving reactions, the reaction-induced fluctuations, the polymer viscoelasticity, and the change in the compressibility of the mixtures during the course of reaction make the problem become theoretically intractable. Here, we have no attempt to apply currently available theories for reaction-induced phase separation in chemical systems, including small molecular mixtures, to analyze the above experimental data. Instead, we estimate the rate of phase separation induced by the cross-link reactions in a phenomenological way based on the concept of linear stability analysis developed for dynamical phenomena.[20,21] In the initial stage of a dynamical process such as phase separation where the linearization process can be applied, the time evolution of the fluctuations $\delta\phi(q,t)$ induced by external perturbation can be approximately expressed by an exponential function of time,

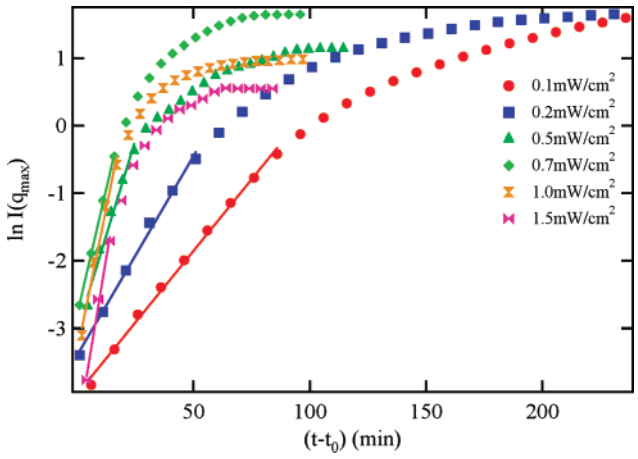

Figure 9. Irradiation time evolution of the scattering peak intensity $I(q_{max})$ obtained for a PSA/PVME (20/80) blend irradiated with various UV intensities.

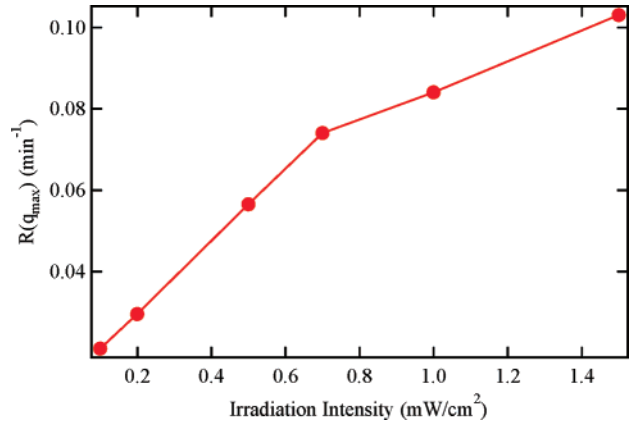

Figure 10. Dependence of the rate $R(q_{max})$ of phase separation on the irradiation intensity calculated from the data shown in Figure 9.

i.e., $\delta\phi(q,t) \sim F(q)e^{R(q)t}$. Here $F(q)$ is a spatially periodic function of the wavenumber q. The exponential part, appearing as the consequence of linearization, characterizes the time evolution of the dynamical process with the growth rate $R(q)$ of a concentration fluctuation having the wavelength $\lambda = 2\pi/q$. In reciprocal space, the scattering intensity $I(q,t)$ from the reacting blend is proportional to the square of this concentration fluctuation $[\delta\phi(q,t)]^2$ and would therefore increase exponentially with irradiation time in the early stage of the reaction-induced phase separation process. From this argument, the linear part of the graph ln $I(q_{max})$ vs t_{irr} at the beginning of the irradiation process may be used as a measure for the rate of phase separation, although unknown are the detailed contribution to fluctuations from cross-linking kinetics, polymer diffusion, reaction-induced increase in molecular weight, its feedback on the dynamics of the system, and the viscoelasticity. The irradiation intensity dependence of the growth rate $R(q_{max})$ calculated from the initial slope of Figure 9 is depicted in Figure 10. It was found that $R(q_{max})$ systematically increases with increasing irradiation intensity and eventually tends to reach a limit at high irradiation intensity. From these experimental results, we conclude that the kinetics of phase separation induced by a photo-cross-linking reaction is quite different from the nonreacting case in two aspects. One is the emergence of the reaction-induced freezing effect that prevents the mixture from approaching phase equilibrium. The other is the decrease in the characteristic length scales ξ with the cross-link time as seen in Figure 8. To confirm that the volume of the cross-linked blend may be greatly changed upon irradiation, Mach−Zehnder

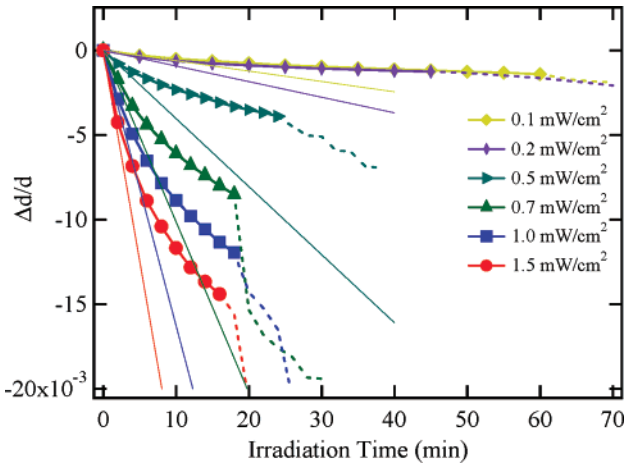

Figure 11. Dependence of the elastic deformation on irradiation time observed at 110 °C for various irradiation intensities in the photo-cross-link process of a PSA/PVME (20/80) blend.

interferometry equipped with a UV light source was employed to in situ monitor the local deformation of the blend along the course of irradiation.[13] Illustrated in Figure 11 is the irradiation time dependence of the elastic strain ($\Delta d/d$) defined in eq 4 observed for a PSA/PVME (20/80) blend irradiated with various light intensities. In the figure, the effects of cross-link on the deformation ($\Delta d/d$) observed in the one-phase region of the blend were indicated by the solid curves for six intensities ranging from 0.1 to 1.5 mW/cm^2. The elastic strain ($\Delta d/d$) decreases with irradiation time, indicating that the photo-cross-linked blend actually shrinks upon cross-linking. It was found that the shrinkage of the blend changes systematically with irradiation intensity, i.e., the greater intensity generates the larger ($\Delta d/d$). As irradiation time exceeds an extent, ($\Delta d/d$) clearly deviates from its course indicated by the solid curves which represent the data of the blend in the miscible region. The irradiation time at which the deviation takes place becomes longer under weaker UV intensity, being in accordance with the absorbance data monitored at 500 nm as depicted in Figure 5. Therefore, this deviation corresponds to the onset of phase separation observed by Mach−Zehnder interferometry. The deformation data obtained after the irradiated blend enters the two-phase region are expressed by the dotted curves in the same figure.

In order to examine the correlation between the "abnormal" evolution of the characteristic length scales ξ with irradiation time in the phase separation process, the irradiation time dependence of ξ shown in Figure 8 was fitted to the following equation:

$$\xi(t) = \xi_0 \exp(-k_\xi t_{irr}) + B \qquad (6)$$

Here, ξ_0 and B are constant, and k_ξ is the shifting rate of the scattering peak which may be used as a measure for the morphological evolution.

On the other hand, the shrinkage process of the blend under irradiation observed by Mach−Zehnder interferometry does not have enough data points for analysis because of the significant intervention of phase separation as illustrated in Figure 11. As a consequence, the initial slope τ_i defined as $\tau_i \equiv d(\Delta d/d)/dt_{irr}$ with $t_{irr} \rightarrow 0$ was used as a measure for the shrinkage process. In order to characterize the deformation process induced by the reaction, the rate of shrinkage k_i is defined as $k_i \equiv 1/\tau_i$. The correlation between the deformation process induced by irradiation cross-link and the time evolution of the characteristic length

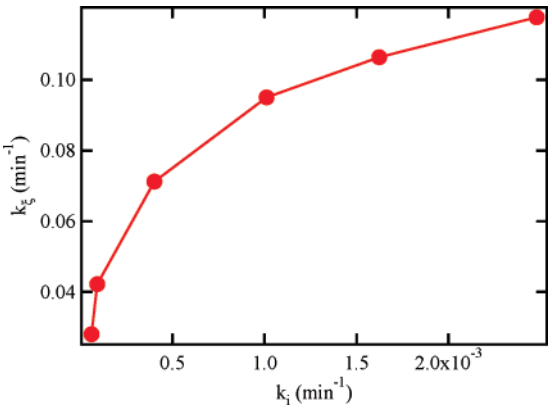

Figure 12. Correlation between the rate of shrinkage measured by Mach−Zehnder interferometer and the shifting rate of the scattering peak obtained for a PSA/PVME (20/80) blend irradiated with 365 nm under six different intensities at 110 °C.

scale ξ of the morphology in these cross-linked blends was examined by plotting k_i vs k_ξ. Though occurring in different time scale, these two kinetics parameters strongly correlate to each other as seen in Figure 12. Namely, the shifting rate k_ξ observed for the scattering peak increases with increasing the shrinking rate $k_i$of the cross-linked blend observed by Mach−Zehnder interferometry and eventually tends to approach a limit at a certain rate of shrinkage as shown in Figure 12. From these experimental results, we conclude that the shrinkage of the blend during the cross-link process would be responsible for the shift of the scattering peaks at q_{max} toward the side of larger wavenumber q.

Reversible Phase Separation of PSA/PVME Driven by Two UV Wavelengths. To examine the reversibility of the phase separation of PSA/PVME blends under alternative irradiation with two different UV wavelengths, a PSA/PVME (20/80) blend was first irradiated over 150 min using 365 nm UV light with the intensity 0.3 mW/cm^2. The light scattering profiles of the blend in this forward (cross-linking) process of phase separation monitored during the course of irradiation are shown in Figure 13a. Similar to the results shown in Figure 6, the scattering peak slowly shifts toward the large q range as phase separation proceeds and eventually becomes almost unchanged after 130 min of irradiation. After 150 min of irradiation under 365 nm, the excitation wavelength was shifted to 297 nm by switching a band-pass filter into the trajectory of the UV beam in the scattering photometer to promote the backward (homogenization) process of phase separation. It was found that upon de-cross-linking the PSAF networks with 297 nm the scattering intensity from the blend gradually decreases with increasing irradiation time as illustrated in Figure 13b. On the other hand, the position of the scattering peak is almost unchanged with irradiation time, indicating that the length scale of the morphology is unchanged while its contrast becomes weakened with irradiation time. These experimental results clearly indicate that the homogenization process has occurred upon de-cross-linking with 297 nm UV light. The details of the reversibility of the cross-link reaction are shown in Figure 4. Displayed in Figure 14a is the time evolution of the characteristic length scales ξ obtained for both the forward and backward processes of the phase separation. ξ decreases with irradiation time in the forward process, whereas it is almost unchanged during the backward process induced by irradiation with 297 nm. On the other hand, as illustrated in Figure 14b, the intensity $I(q_{max})$of the scattering peak increases with irradiation time under 365 nm and then decreases upon switching the wavelength to 297 nm for the backward process. These experimental results indicate that phase

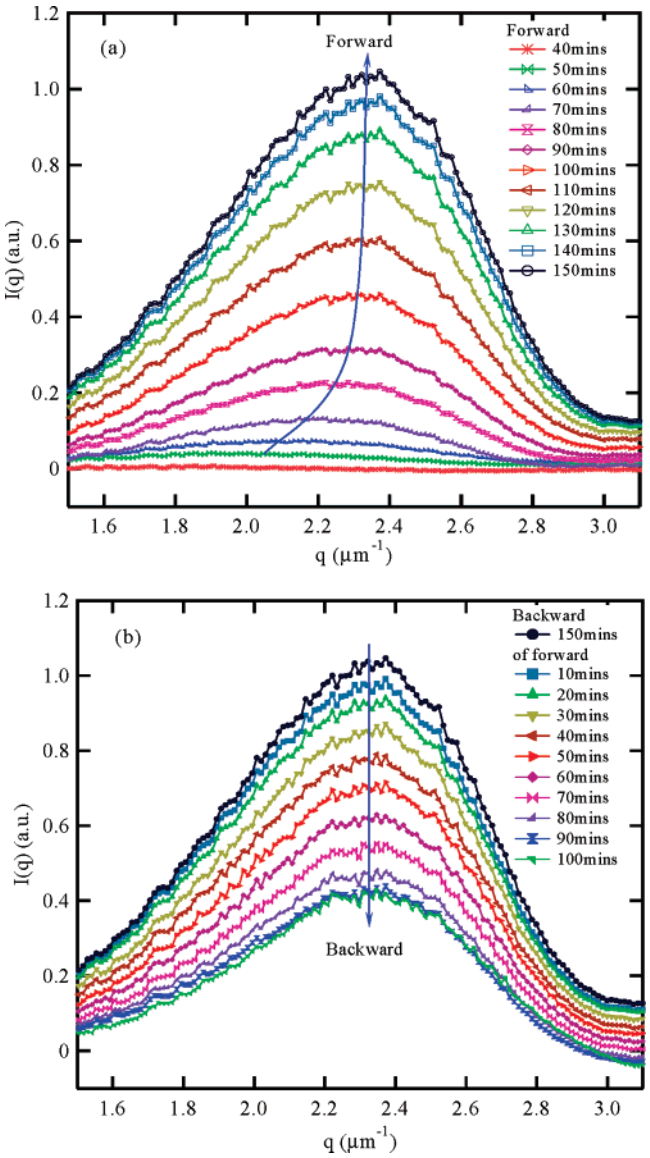

Figure 13. (a) Evolution of the scattering intensity with irradiation time in the forward process promoted by UV light (365 nm, 0.3 mW/cm^2) at 110 °C. (b) The backward process induced by irradiation with shorter UV light (297 nm, 0.5 mW/cm^2) observed at the same temperature.

separation of the PSA/PVME (20/80) blend can be reversibly induced by two UV wavelengths 365 and 297 nm. The insensitivity of the position of q_{max} to the irradiation time in the backward process would originate from the following two reasons. One is the overlap between the absorption spectra of anthracene and its photodimer at the wavelengths used to induce homogenization. It should be noted that the extinction coefficient of anthracene is small but nonzero ($\epsilon \cong 600$ cm^{-1} M^{-1}) at 297 nm.[22] The other is the very high viscosity arising from the cross-link networks. Nevertheless, the homogenization of the blend induced by 297 nm can be clearly observed in the change of the scattering profile illustrated in Figure 13b. In principle, increasing the intensity at 297 nm or using laser with tunable wavelengths could lead to a more efficient control of the reversibility. The experimental results described here indicate that phase separation of the PSA/PVME blend can be reversibly driven by using two UV wavelengths, and the efficiency of the reversible control of phase separation would depend strongly on the selection of the two excitation wavelengths. It should be noted that reversible photodimerization has been demonstrated

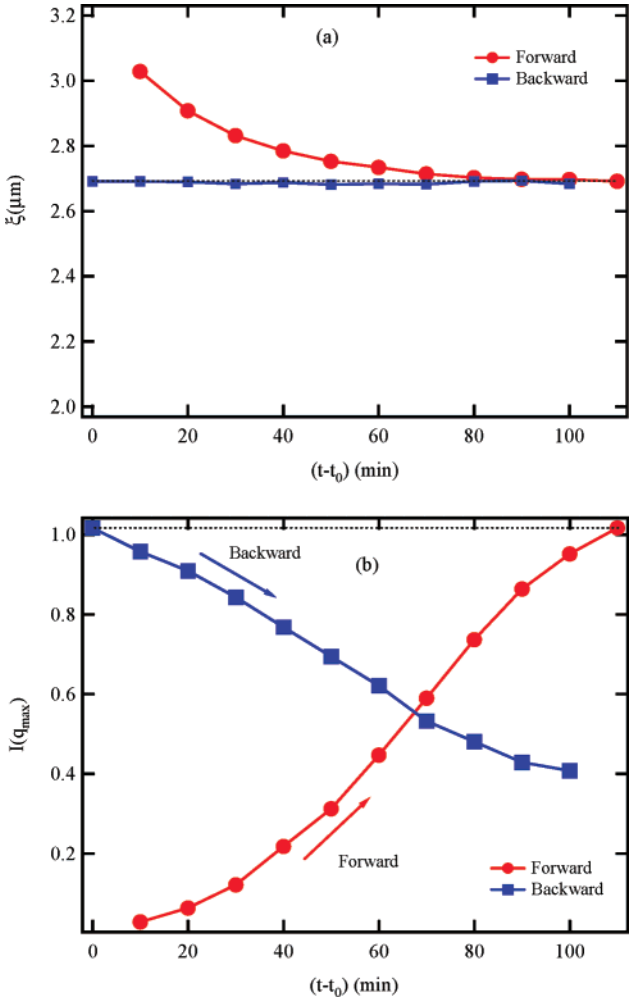

Figure 14. Time evolution of the characteristic length scale of the morphology (a) and the peak intensity (b) obtained in the forward and backward processes shown in Figure 13a,b.

to trigger the transition from microphase to macrophase separation of poly(styrene)-*block*-poly(methyl methacrylate) by taking advantages of photocleavage of the anthracene photodimers used as a junction between the polystyrene and poly(methyl methacrylate) components of the diblock.[23] Most recently, reversible photodimerization of coumarin was also used to stabilize polymer micelles.[24]

On the Time Evolution of the Phase Separation Observed by Light Scattering. It is worth noting that the scattering behavior similar to those shown in Figures 6 and 13a for the forward process of phase separation was also reported previously in a kinetic study of phase separation in cured epoxy systems.[25] Depending upon the composition of the epoxy resin, the time evolution of the scattering profiles could exhibit the "normal" behavior; i.e., the scattering peak moves to the side of small wavenumber q or unusually shifts to the opposite (large q) side. This peculiar kinetics of phase separation was ascribed to the nucleation-initiated spinodal process arising from the change of the phase diagram with the curing reaction. Here, we took a different approach by considering the fact that considerable change in volume of the blend was induced by the cross-linking reaction of the PSA component. Therefore, interferometric experiments were performed in situ to confirm the effects of deformation associated with this reaction. The elastic deformation shown in Figure 11 obtained by the in situ experiments using Mach−Zehnder interferometry provides clear evidence for the shrinkage of the PSA/PVME (20/80) blend generated

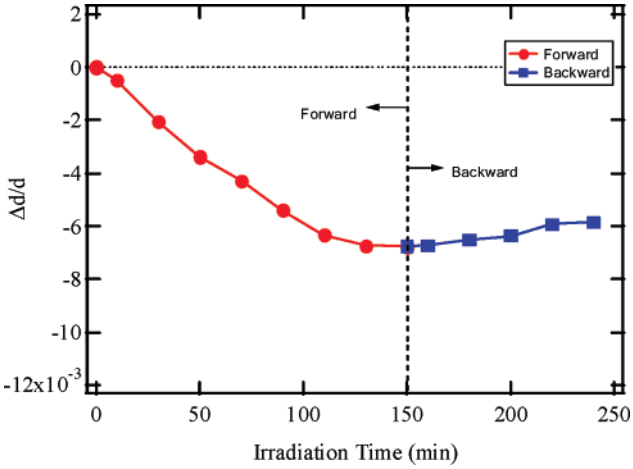

Figure 15. Elastic deformation of a PSA/PVME (20/80) blend cross-linked by irradiation with 365 nm (0.3 mW/cm^2) in 150 min and subsequently de-cross-linked by 297 nm (0.5 mW/cm^2) in 100 min. The experimental temperature is 90 °C in the one-phase region.

by the photo-cross-link process. Furthermore, the effects of volume shrinkage on the evolution of the morphology monitored during irradiation are also supported by the close correlation between the two kinetic parameters k_ξ and k_i illustrated in Figure 12.

Recently, it was found from interferometric studies on photo-cross-linked blends that there exist three types of strain relaxation depending on the cross-link density.[13,26] For the case of low cross-link density, the deformation generated by the reaction slowly recovers after stopping irradiation because the sample does not yet enter its glassy state. However, as the cross-link density reaches a certain threshold, the volume recovery disappears, and the dimension of the irradiated blend is apparently unchanged within the time scale of the experiment due to glassification. Further increase in cross-link density results in an additional shrinkage of the blend at long time, reflecting the aging phenomena in the glassy state of the cross-linked blend. As a consequence, the shift of the scattering peak observed by light scattering would depend on the composition and particularly on the cross-link density of the blend. For the experimental conditions used in this study, the shift of the scattering peak toward the large q side would be mainly caused by the contraction of the blend by cross-link.

On the other hand, for the homogenization process induced by irradiation with 297 nm, the scattering intensity significantly decreases while the scattering peak is almost unchanged with irradiation time. These results are in good agreement with the deformation data obtained by Mach−Zehnder interferometry under the same irradiation conditions. As illustrated in Figure 15, a PSA/PVME (20/80) blend exhibits shrinkage after photo-cross-link by irradiation with 365 nm (0.3 mW/cm^2) in 150 min and subsequently shows almost no deformation after de-cross-link under 297 nm (0.5 mW/cm^2) in 100 min. These results suggest that the photo-cross-linked blend did not undergo significant deformation in the de-cross-link process using 297 nm. Taking into account that the recovery of anthracene monomer can be performed with a good efficiency as evidenced in Figure 4, and there is also a close correlation between the temporal behavior of the scattering from the blend irradiated with 365 nm and the time dependence of the deformation monitored in situ by Mach−Zehnder interferometry, we may conclude that the elastic contraction of the blend induced by the photo-cross-link reaction is mainly responsible for the "unusual" scattering behavior observed in Figures 6 and 13a.

Many years ago, Han and co-workers performed reverse temperature-quench experiments for a polystyrene/poly(vinyl methyl ether) blend using light scattering. They found that the scattering peak moves toward the small q direction while its intensity decreases with time during a temperature drop from the spinodal into the miscible region.[27] These results are in contrast with the data obtained by reversible photo-cross-link shown in this study. The reason responsible for the difference between the behavior of phase separation in these two systems is that for a given reacting mixture the phase diagram changes with the reaction yield. As a consequence, there may exist a particular free energy function corresponding to each reaction yield, whereas there is only one free energy function determined by the composition of the blend for nonreactive mixtures. In principle, the mixture can go back and forth between two different free energy curves if the reversibility of the reaction can be well controlled. For our conditions, the scattering peak does not change during the homogenization process because of the high cross-link density of the blend and also the limitation caused by the overlap of the absorption of anthracene and its photodimer at the excitation wavelengths used to promote the forward and backward reactions. If appropriate wavelengths can be chosen, the scattering peak would trace back the trajectory along which the phase separation proceeds because the system tries to go back to the state corresponding to the initial free energy function. This particular feature discriminates the reacting blends from the nonreacting ones. Finally, from the practical viewpoint, one may take advantage of this reversibility of phase separation to develop the idea of designing "photorecyclable" polymer blends without using solvents to mix or dissolve the two polymer components. Further experiments using different wavelengths for irradiation and other reversible photochemical reactions are currently in progress to elucidate the feature of light-induced reversible phase separation.

Conclusions

In this paper, the following experimental results were obtained for the reversible phase separation of polystyrene derivatives/poly(vinyl methyl ether) blends driven by two different UV wavelengths taking advantages of photodimerization and photodissociation of anthracene.

(1) Upon irradiation with 365 nm UV light, anthracene moieties labeled on polystyrene undergo photodimerization, leading to phase separation between the two polymers. Light scattering data exhibit the unusual time evolution process with the peak shifting toward the side of large wavenumber and eventually reaching a stationary state. On the other hand, irradiation with 297 nm leads to the homogenization of the phase-separated blends as revealed by a decrease in the scattering intensity with increasing irradiation time.

(2) The elastic deformation of the photo-cross-link blend observed in situ by Mach−Zehnder interferometry exhibits a strong correlation between the strain relaxation induced by the cross-link reaction and the time evolution of the morphological length scales. These results suggest that the elastic strain generated by the cross-link reaction plays an important role in the phase separation kinetics of cross-linked systems and also affects the time evolution of the light scattering intensity.

(3) The polymer blends described in this work could provide an idea to design a model system for photorecycling using two different UV wavelengths. These results also suggest that photorecycling of multicomponent polymers would become practical if an appropriate set of excitation wavelengths could be selected to promote the forward and backward processes of anthracene and its photodimer in the blend.

Acknowledgment. This work is financially supported by the Ministry of Education (MONKASHO), Japan, through the Grant-in-Aid No. 16072210 on the Priority-Research-Area "Molecular NanoDynamics". X.-A. Trinh thanks MONKASHO for the scholarship to pursuit the Ph.D program at Kyoto Institute of Technology, Japan.

References and Notes

(1) See, for example: *Nanobiotechnology: Concepts, Applications and Perspectives;* Niemeyer, C. M., Mirkin, C. A., Eds.; Wiley-VCH: New York, 2004.

(2) For example, see: Vicsek, T. *Fluctuations and Scaling in Biology*; Oxford University Press: Oxford, 2001.

(3) (a) Tran-Cong, Q.; Kawai, J.; Endoh, K. *Chaos* **1999**, *9*, 298−307. (b) Tran-Cong-Miyata, Q.; Nishigami, S.; Yoshida, S.; Ito, T.; Ejiri, K.; Norisuye, T. In *Nonlinear Dynamics in Polymeric Systems;* Pojman, J. A., Tran-Cong-Miyata, Q., Eds.; ACS Symp. Ser. 869; American Chemical Society: Washington, DC, 2004; Chapter 22, pp 276−290.

(4) For example, see: (a) Irie, M. *Adv. Polym. Sci.* **1990**, *94*, 27−67. (b) Ichimura, K. *Chem. Rev.* **2000**, *100*, 1847−1873. (c) Ikeda, T.; Tsutsumi, O. *Science* **1995**, *268*, 1873−1875.

(5) *Polymers as Electro-optical and Photo-optical Active Media*; Shibaev, V. P., Ed.; Springer-Verlag: Berlin, 1996.

(6) *Techniques of Chemistry*; Brown, G. H., Ed.; Wiley-Interscience: New York, 1971; Vol. III.

(7) (a) Ohta, T.; Urakawa, O.; Tran-Cong, Q. *Macromolecules* **1998**, *31*, 6845−6854. (b) Urakawa, O.; Yano, O.; Tran-Cong, Q.; Nakatani, A. I.; Han, C. C. *Macromolecules* **1998**, *31*, 7962−6854.

(8) See, for example: Kagan, J. *Organic Photochemistry: Principles and Applications*; Academic Press: New York, 1993; Chapter 8.

(9) Paik, C. S.; Morawetz, H. *Macromolcules* **1973**, *5*, 171−177.

(10) (a) Victor, J. G.; Torkelson, J. M. *Macromolecules* **1987**, *20*, 2241−2250. (b) Yu, W. C.; Sung, C. S. P.; Robertson, R. E. *Macromolecules* **1988**, *21*, 355−364.

(11) Mita, I.; Horie, K.; Hirao, K. *Macromolecules* **1989**, *22*, 558−563.

(12) (a) Yoshizawa, H.; Ashikaga, K.; Yamamoto, M.; Tran-Cong, Q. *Polymer* **1989**, *30*, 534−539. (b) Kataoka, K.; Harada, A.; Tamai, T.; Tran-Cong, Q. *J. Polym. Sci., Polym. Phys.* **1998**, *36*, 455−462.

(13) Inoue, K.; Komatsu, S.; Trinh, X.-A.; Norisuye, T.; Tran-Cong-Miyata, Q. *J. Polym. Sci., Polym. Phys.* **2005**, *43*, 2898−2913.

(14) Tran-Cong-Miyata, Q.; Nishigami, S.; Ito, T.; Komatsu, S.; Norisuye, T. *Nat. Mater.* **2004**, *3*, 448−451.

(15) Harada, A.; Tran-Cong, Q. *Macromolecules* **1997**, *30*, 1643−1650.

(16) Stein, R. S.; Keane, J. J. *J. Polym. Sci.* **1955**, *17*, 21−44.

(17) Tien, P. K.; Ulrich, R. *J. Opt. Soc. Am.* **1970**, *60*, 1325−1337.

(18) For the composition PSA/PVME (20/80), it was found that the refractive index of the blend before irradiation at 22 °C is n =1.487 10, and the maximum change in the refractive index of the irradiated blend is $\Delta n = 1.8 \times 10^{-4}$ for various irradiation conditions indicated in Figure 10. Thus, $\Delta n \cong 0$ can be used as an approximation to derive eq 3.

(19) For example, see the early works on phase separation kinetics of polymer blends: (a) Nojima, S.; Tsutsumi, K.; Nose, T. *Polym. J. (Tokyo)* **1982**, *14*, 225−232. (b) Hashimoto, T.; Kumaki, J.; Kawai, H. *Macromolecules* **1983**, *16*, 641−648. (c) Snyder, H. L.; Meakin, P.; Reich, S. *Macromolecules* **1983**, *16*, 757−762.

(20) Nicolis, G.; Prigogine, I. *Self-Organization in Nonequilibrium Systems*; John Wiley and Sons: New York, 1977; Chapter 6.

(21) Cross, M. C.; Hohenberg, P. *Rev. Mod. Phys.* **1993**, *65*, 851−1112.

(22) Berlman, I. B. *Handbook of Fluorescence Spectra of Aromatic Molecules*; Academic Press: New York, 1971.

(23) Goldbach, J. T.; Lavery, K. A.; Penelle, J.; Russell, T. P. *Macromolecules* **2004**, *37*, 9639−9645.

(24) Jiang, J.; Qi, B.; Lepage, M.; Zhao, Y. *Macromolecules* **2007**, *40*, 790−792.

(25) Kyu, T.; Lee, J.-H. *Phys. Rev. Lett.* **1996**, *76*, 3746−3749.

(26) Takeda, S. Master Dissertation, Department of Polymer Science and Engineering, Kyoto Institute of Technology, March 2006, to be published.

(27) Akcasu, A. Z.; Bahar, I.; Erman, B.; Feng, Y.; Han, C. C. *J. Chem. Phys.* **1991**, *97*, 5782−5793.

MA0705220